Experimental study of molecular and cluster effects in secondary electron emission

Hermann Rothard, Kurt Kroneberger, Erling Veje,* Alexander Clouvas,† Jürgen Kemmler, Peter Koschar, Norman Keller, Sergio Lencinas, Peter Lorenzen, Oliver Heil, Dieter Hofmann, and Karl-Ontjes Groeneveld
Institut für Kernphysik, Johann-Wolfgang-Goethe-Universität, August-Euler-Strasse 6, D-6000 Frankfurt am Main 90, West Germany
(Received 1 September 1989)

We have measured the ion-induced secondary-electron-emission (SEE) yields in forward and backward directions from thin sputter-cleaned foils in ultrahigh vacuum. C, Al, Ti, Ni, and Cu have been bombarded with H^+, H_2^+, and H_3^+ (0.3–1.2 MeV/amu), and C and Al have been bombarded with C^+, O^+, and CO^+ (15–85 keV/amu). The yields induced by molecular and cluster ions are compared to those induced by the corresponding isotachic monoatomic projectiles. We observe molecular effects as yield reductions at low projectile velocities ($v_p \approx v_o$) and yield enhancements at higher velocities ($v_p \gg v_o$). The results are discussed in the framework of the extended kinetic-emission model by Sternglass and the energy-loss model for clusters by Brandt and Ritchie. The velocity dependence of the molecular effect in SEE follows the velocity dependence of the molecular effect in Brandt's energy-loss calculations. Thus it seems that the energy loss is also proportional to SE yields for molecular projectiles at velocities around and above the Bohr velocity v_0.

I. INTRODUCTION

It is well established that the interaction between heavy, swift atomic particles and a solid can result in emission of electrons from the target surface. This is referred to as secondary electron emission (SEE), and the total SEE yield, γ, is defined as the average number of electrons emitted per incoming projectile.

Different production mechanisms lead to SEE.

(i) The so-called kinetic emission of electrons is generally considered as a three-step process. First, the projectile transfers kinetic energy to target electrons. Next, a fraction of these electrons moves from the bulk towards the target surface, and, finally, a fraction of the electrons reaching the surface passes through it. Thus, the kinetic emission is clearly related to that fraction of the kinetic energy of the projectile which is communicated to target electrons (the electronic stopping power, dE/dx), and Sternglass[1] suggested γ to be proportional to dE/dx.

(ii) If the neutralization energy of the projectile at the target surface is more than a factor of 2 larger than the work function of the target material, an electron may be ejected from the target at the same time as another target electron is captured by the projectile.[2] This is essentially an Auger transition, and is referred to as potential SEE. Being exothermic, it can occur for all projectile energies, as long as conservation laws are not violated, and it is generally assumed to be a steadily decreasing function of the projectile energy. However, potential ejection can be the primary source for SEE only at projectile energies substantially lower than those used in the present work and therefore is disregarded in the following discussion.

(iii) For heavy projectiles at not very low energies, recoiling target atoms can also cause kinetic SEE with the result that a fraction of γ is related to the nuclear stopping power, see, e.g., Ref. 3. Since this fraction is very small, it shall be disregarded in the following.

However, it must be kept in mind that a full, quantitative theoretical description will be very involved, being a many-body problem to be solved by time-dependent quantum mechanics. This makes an *ab initio* theory difficult at present and calls for systematic experimental studies.

Some experimental studies[4–13] have been carried out to test whether a possible proportionality between γ and the electronic stopping power exists. This proportionality was confirmed experimentally as a function of the projectile velocity v_p for proton bombardment in a wide energy range $10\ \text{keV} \le E_P \le 10\ \text{MeV}$.[13–15] With heavy ions, some deviations from this simple proportionality, especially at low projectile velocities ($E_p/M_p < 200$ keV/nucleon), have been observed.[3,12,16] For a recent review of data obtained with protons see Refs. 13 and 14, and for a discussion of heavy-ion-induced SE yields from thin foils see Ref. 12.

A few experiments[17–21] have been carried out with incoming molecular ions besides isotachic monoatomic projectiles with the task to answer the question of whether the SEE yield produced by a molecular projectile equals the sum of SEE yields produced by the atomic constituents of the molecule. Conveniently, the "molecular effect" is expressed by the ratio R between the yield induced by the molecule and the sum of the yields produced by its constituents:

$$R(\gamma) = \frac{\gamma(\text{molecule})}{\sum \gamma(\text{atomic constituents})} \tag{1}$$

and thus, an observation of $R \neq 1$ is taken as an indication of the presence of a molecular effect.

Molecular effects have been observed in other features related to atom-solid interactions such as charge-state distributions (see Refs. 22–25 and references quoted therein), optical beam-foil processes (see Refs. 25 and 26

 ©1990 The American Physical Society

and references therein), and also in energy-loss measurements.[27–30] Of these various phenomena for which molecular effects can be present, we want here to call special attention to the energy-loss processes, because, as mentioned above, according to the model of Sternglass,[1] one would expect proportionality between γ and the electronic stopping power.

Stopping powers have been measured with molecular projectiles only in rare cases, and enhancements ($R>1$) as well as reductions ($R<1$) have been reported.[27–31] Yet the available data are too sparse to unravel systematic trends, though it comes out that the stopping power for a molecule is a function of the velocity of the projectiles as well as of the orientation of the cluster with respect to the direction of motion.[27–34] Therefore, conversely, if a proportionality between γ and dE/dx, as predicted by Sternglass,[1] is confirmed experimentally, SEE data can yield valuable information in cases where stopping-power measurements are difficult or uncertain. This indicates the need for further experimental studies of SEE as well as stopping powers with molecules. However, we mention that it is not clear at all whether one should expect γ to be proportional to dE/dx for the molecular projectiles used here, because at the lowest projectile energies a strict proportionality between γ and dE/dx does not seem to be fulfilled even for the corresponding monoatomic projectiles.[11,12]

For molecular projectiles, the number of electrons can differ from the total number of electrons of the corresponding monoatomic projectiles. Therefore, a question related to molecular phenomena is the charge-state dependence of SEE induced by monoatomic projectiles as well as the SE yield induced by electrons. For example, the question can be raised of whether a neutral projectile produces secondary electrons in an amount equal to the sum of those produced by a singly ionized positive ion and an isotachic electron.[23,35] According to Ref. 36, it is normally expected, but not well documented experimentally, that isotachic protons and electrons produce the same number of secondary electrons. However, Ref. 36 refers only to a few not very convincing data sets. Furthermore, Hölzl and Jacobi[37] have measured SEE produced by 0.1–1 keV electrons. Their data together with those given in Ref. 21 seem to indicate that the yield produced by electrons is only approximately 0.6 times the yield produced by isotachic protons, but firm conclusions cannot be drawn from these data sets,[21,35,37] because they have been obtained under different experimental conditions. Thus, one might expect neutral hydrogen atoms (H^0) to produce from around 1.6 to 2 times as large a yield of secondary electrons as isotachic H^+.

Kroneberger *et al.*[21] studied the secondary-electron yields produced both in forward (γ_f) and in backward (γ_b) directions by H^0 and H^+ traversing thin carbon foils. They found that $\gamma_f(H^0)\approx 2\gamma_f(H^+)$ for the thinnest foil they used, decreasing towards $\gamma_f(H^0)=\gamma_f(H^+)$ with targets thicker than ~ 250 Å and $\gamma_b(H^0)\approx 1.6\gamma_b(H^+)$. However, these data were taken only at one relatively high energy (1.2 MeV/u), whereas in the present paper we report on energies as low as 15 keV/u. Thus, again, the need for experimental studies of SEE induced by isotachic protons, electron-carrying projectiles (like molecules, clusters, and heavy ions) and electrons within the same detection system for velocities around and above the Bohr velocity becomes obvious.

II. EXPERIMENT

The experiments were carried out in the UHV chamber at the 2.5-MV Van de Graaff accelerator at the J. W. Goethe Univeristy in Frankfurt, Germany, described in Ref. 38. The pressure during the measurements was $p_{UHV}<2\times 10^{-7}$ Pa. Special equipment for the measurement of the SE emitted in the forward and backward directions was installed in this chamber, as shown in Fig. 1. Two stainless-steel cylinders (no. 3), the so-called "γ cups," with a conical opening towards the target (no. 4), collected the emitted SE independently in the forward and backward directions.

Grids (no. 2) at the front of both cylinders were held at a negative potential to avoid the collection of SE produced outside the "γ- cups," e.g., at the apertures, and to hold back the fast SE emitted downstream. The beam could pass these high-transmission grids through small holes without producing SE. By applying a positive potential to the γ cups, the SE could be completely collected. A negative potential applied to the target helped to avoid influences due to instabilities of the beam intensity or contact potentials (see, e.g., Ref. 21).

With symmetric potentials of $+40$ V at the γ cups and -40 V at the target holder and grids, the sum of the SE collected in the cups in the forward and backward directions, i.e., $\gamma_f+\gamma_b$, was equal to the total SE yield, γ_t (which can easily be obtained by measuring the ion-induced target current[21]) within $\pm 5\%$. Furthermore, the ratio of the forward to the backward SE yield, $R=\gamma_f/\gamma_b$, showed the same value as measurements with other equipment[21] within an error of $\pm 8\%$. The collection of SE from the apertures was also minimized by applying a positive potential ($+80$ V) to a beam aperture in front of the target.

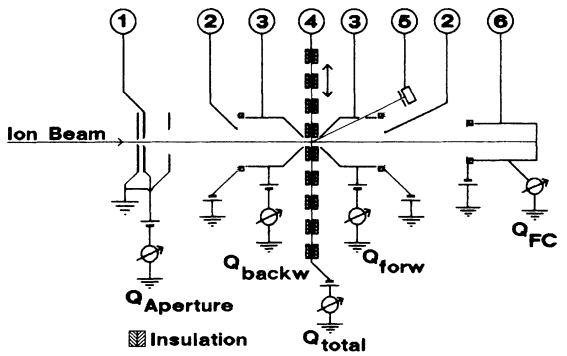

FIG. 1. Experimental setup. (1) Antiscattering and beam-current-normalization aperture, (2) electron repelling grids, (3) "γ cups" which collect the secondary electrons emitted in the forward and backward directions, (4) target holder with eight targets, (5) particle detector for scattered projectiles, (6) Faraday cup with electron repeller.

We used thin, self-supporting target foils of C, Al, Ni, Ti, and Cu produced by standard evaporation methods. The pressure during the evaporation was held at 2×10^{-5} Pa, using a diffusion pump with an LN_2 trap in order to achieve foils that are as pure as possible. The foils were held by rectangular frames with $\phi=10$-mm holes, mounted on a target holder (no. 4 in Fig. 1) connected to a UHV linear motion feedthrough. In this way, eight different targets could be alternately moved into the beam axis.

A UHV-compatible charged-particle detector (no. 5) mounted at an observation angle of 35° with respect to the beam axis could measure elastically scattered projectiles through a small hole in the forward γ cup. The target thickness of the C and Al target foils was then calculated relative to the count rate from optically calibrated "normalization" foils of a 1000-Å thickness each for C and Al. With Ni, Ti, and Cu we used only a few foils each and their thickness was measured during evaporation using a standard quartz oscillator technique. The smallest foil thicknesses were 160 Å for Al and 145 Å for C.

The beam, which was prepared by the 2.5-MV Van de Graaff Accelerator, was momentum analyzed in a magnet and deflected by 15° into the beam line, where the pressure was 10^{-4} Pa. The beam was focused by several apertures over a distance of 5 m to a diameter of <1 mm on the target and then collected in the Faraday cup (no. 6). Unfortunately, we have no opportunity to check on how pure the molecular beams were, but from known breakup cross sections[39] we can estimate that only a fraction of $<5\%$ of the molecular beam, which might be broken up in the beam line between the separation magnet and the target, could reach the target and cause a systematical error of up to 5%.

Before the measurements with H^+, H_2^+, and H_3^+, the targets were cleaned by sputtering with heavy noble-gas ions.[40] In the case of the C^+, O^+, and CO^+ projectiles, the targets were sputter cleaned with slow CO^+. The residual target surface contaminations could be controlled in the following ways.

(i) By measuring the total SE yield γ_t. The decrease of γ_t towards a saturation value during sputtering due to an increase of the work function and a reduction of the SE escape depth when adsorbates and oxides are sputtered away and the surface roughness is smoothed (see Refs. 16 and 40–42) is a simple method for surface control. A minimum γ_t value indicates an optimum cleaned surface.

(ii) By means of Rutherford forward-scattering methods using the particle detector (no. 5). This offers a possibility to control the composition and contamination of both the surface and the bulk of the target which is sensitive to different elements. We estimate the residual contamination with C and O to be (much) lower than 0.1 monolayer.

The number of SE collected in the γ cups was usually normalized to the beam current collected in the Faraday cup (FC no. 6 in Fig. 1) behind the target. With the slow, heavy ions and molecular projectiles this was not possible, since, due to the strong multiple scattering of the slow ions and the Coulomb explosion of the molecular projectiles, the beam was broadened up and could no longer be fully collected in the FC. In these cases we used the antiscattering aperture (no. 1 in Fig. 1) as a beam monitor and normalized to the current collected there. For the normalization to the number of projectiles, the ratio of the currents at the aperture and in the FC was measured without a target between each run with a target. The experimental error of $\pm8\%$ with FC normalization increased to $\pm15\%$ with the aperture normalization.

III. RESULTS AND DISCUSSION

A. Data obtained with hydrogen molecular projectiles

In Fig. 2 the SE yields γ_f (left) and γ_b (right) obtained with H^+, H_2^+, and H_3^+ at 0.3 MeV/u are plotted versus the target thickness of the aluminum foils. We generally observe that γ_f is a factor of 1.1 up to 1.2 larger than γ_b. Similar findings have been reported previously.[9,43] This can be interpreted by the fact that binary collision processes will clearly favor SEE in the forward direction.

As can be seen from the figure, our data do not show (within the uncertainty limits) a systematic dependence of te SE yields γ_f and γ_b on the foil thickness within the target thickness range used here. SEE can be associated with the following mean free paths (MFP) which must be put in relation to the target thickness d.

(i) The MFP for charge exchange of the projectile, λ_c.

(ii) The MFP for electrons escaping from the solid into the vacuum, $\lambda_e(E_e)$. Since the majority of emerging electrons has energies around $E_e\approx10$ eV, we have an escape depth or average MFP $\lambda_e(E_e=10\text{ eV})\approx15$ Å. A more thorough discussion is found in Ref. 44.

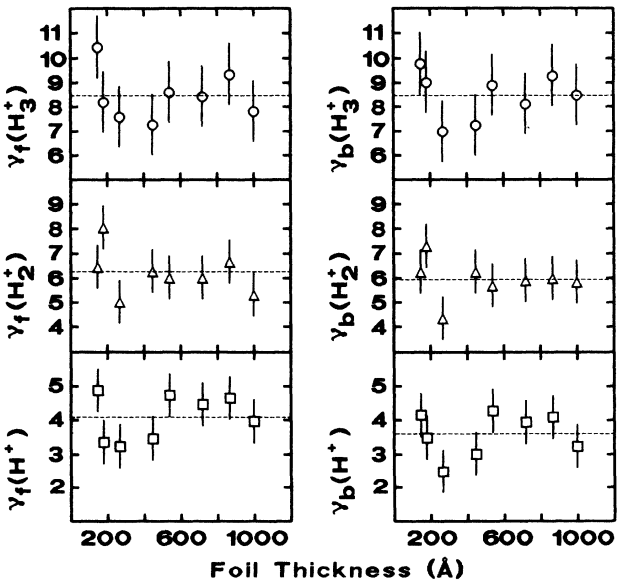

FIG. 2. Data for γ_f (left-hand side) and γ_b (right-hand side) obtained with H^+, H_2^+, and H_3^+ at 0.3 MeV/u in aluminum targets, plotted vs the foil thickness. The dashed lines indicate the values γ_f and γ_b, averaged over the foil thickness, for each projectile.

Thus, the behavior of the backward SE yields can be understood by the fact that the foil thickness $d > 150$ Å was always larger than the escape depth of the SE, which is in the order of $\lambda_e \approx 10-20$ Å,[44] and thus $\lambda_e \ll d$. Also, the binding electrons are stripped off within the first 50–100 Å (Ref. 45) of the target foil, i.e., within the MFP for charge exchange λ_c, which again is smaller than the thinnest foils used: $\lambda_c < d$.

In the forward direction, however, a target thickness dependence of γ_f in a comparable target thickness range has been reported in the case of carbon foils.[21] This dependence was interpreted as a molecular effect, which decreased with increasing target thickness due to the increasing separation between the cluster particles, caused by Coulomb explosion of the molecule and multiple scattering. Similar results have been reported as well for stopping powers[28] in charge-state distributions,[22] optical beam-foil excitation measurements,[25] and in quantum beat studies.[26] However, all molecular effects under study have been found to decrease steadily with increasing foil thickness d and to be very small or absent at dwell times comparable to the longer ones in our experiment.

In our experiment, however, for the heavier target materials and lower projectile velocities the multiple scattering is stronger, destroying the correlation between the constituents of the molecular projectile already at a smaller target thickness. In these cases, a target thickness dependence of γ_f due to a molecular effect would be expected to take place in a target thickness range below the thinnest foils we could use. For our discussion below, we therefore use the mean SEE yields, averaged over the foil thickness.

In Fig. 3 the mean values of γ_f (left) and γ_b (right) for protons (upper part) are plotted versus the projectile energy per proton for different target materials (C, Al, Ti, Ni, and Cu). In the lower parts of the figure, the ratios $R(\gamma_f)$ [Eq. (1)] (left) and $R(\gamma_b)$ (right) are plotted for H_2^+ (middle part) and H_3^+ (lower part), respectively. The dashed lines indicate $R=1$, where the yield of the molecule would equal the sum of yields of its atomic constituents and thus signalize the "no molecular effect" value.

For H_2^+, the forward ratio is slightly below unity, i.e., $R_f = 0.85 \pm 0.15$, and shows no significant dependence on the projectile energy. Since, as seen from the above discussion, no molecular effect is expected for γ_f, this might indicate a systematical error of 15% for $R(\gamma_f)$.

In the backward direction, however, a slight increase of $R(\gamma_b)$ with E_p can be seen, starting with $R \approx 0.75 \pm 0.15$ (<1) at 0.3 MeV/u and ending with $R \approx 1.2 \pm 0.15$ (>1) at 1.2 MeV/u for most target materials. A new result is that we observe a reduction of the SEE yield per proton for hydrogen clusters at low velocities ($v_p < 5\ v_o$).

Kroneberger *et al.*[21] studied SEE with H^0, H^+, and H_2^+ projectiles at 1.2 MeV/u using thin carbon foils and found an enhancement of $R(\gamma_b) \approx 1.2$. They interpreted this as a proportionality between the molecular enhancement in the SEE yield and electronic stopping power for

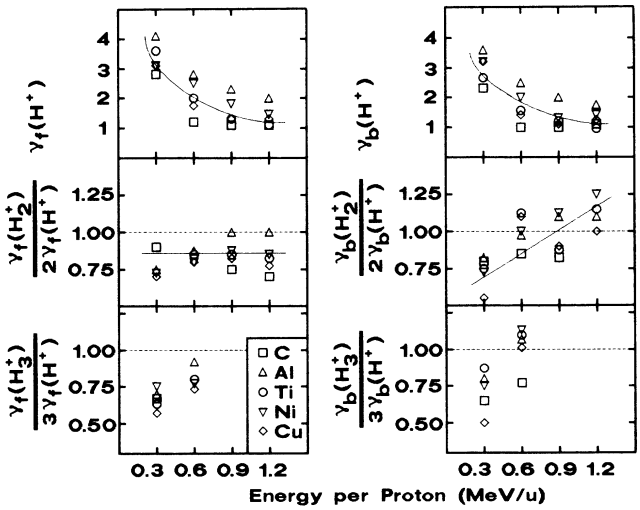

FIG. 3. In the top section γ_f (left-hand side) and γ_b (right-hand side) obtained with H^+ and five different target materials (C, Al, Ni, Ti, and Cu) are plotted vs the projectile energy. Below are plotted the ratios $R(\gamma_f)$ (left-hand side) and $R(\gamma_b)$ (right-hand side) between the SEE yields induced by the molecular projectiles and the sum of yields induced by two, respectively, three protons for H_2^+ (middle section) and H_3^+ (bottom section), respectively, vs the projectile energy per proton. The lines are drawn to guide the eye. The dashed lines indicate $R=1$, i.e., no molecular effect, see text.

H_2^+ in accordance with the Sternglass model.[1]

The electronic stopping power per proton for H_2^+ and H_3^+ at velocities relevant to this work has been measured on carbon and gold foils and found to be somewhat (factors of approximately 1.2 and 1.5, respectively) larger than those for H^+ (Ref. 27). This was related to the well-known fact that the electronic energy-loss scales with the square of the effective charge of the projectile, implying that for distant interactions the protons forming a cluster will act almost as a point projectile with a charge equal to the sum of the charges of the protons, whereas for close interactions the protons will act independently.[27]

On the other hand, a stopping-power ratio smaller than 1 has been reported for slow H_2^+ and N_2^+ in carbon.[31,46] The "molecular effect" R changes from a reduced ($R<1$) to an enchanced value at a velocity around one atomic unit. Thus, it is, in principle, possible for H_2^+ and H_3^+ that corresponding reductions of the stopping powers are present at the velocities where we observe molecular and cluster reductions in the SEE yields.

Furthermore, in H_2^+ and H_3^+ clusters, the charge of the cluster will be screened by the binding electrons. This will lead to a reduced stopping power and SE production just within the first few nm of the foil, from which the SE emitted in backward direction originate. The slower the projectile is, the less the binding electrons can contribute to γ_b, so that the screening dominates, causing $R(\gamma_b) < 1$.

With H_3^+, similar conclusions can be drawn from our results. Although we could measure at only two energies

of 0.3 and 0.6 MeV/u, the data show the same trend as with H_2^+, namely an increase of γ_b with the projectile energy. A slight increase of γ_f with E_p can be seen, which is not expected to be significant, see discussion above.

B. Data obtained with CO^+

The values for γ_f and γ_b, measured with CO^+ projectiles on carbon targets of various thicknesses, are plotted versus the projectile energy per nucleon in Fig. 4. For comparison, the sums of $\gamma_{f,b}$ obtained with monoatomic projectiles (C^+ and O^+) are also shown. The corresponding data obtained with Al foils are given in Fig. 5. We note from these two figures that the SEE yields produced by CO^+ are mainly somewhat (say, 15%) smaller than the sum of yields produced by C^+ and O^+, and that, again, there is no clear monotonic variation with foil thickness. The R values [Eq. (1)] corresponding to the data given in Figs. 4 and 5 are shown in Fig. 6, but since no clear variation of $\gamma_{f,b}$ with foil thickness is seen in Figs. 4 and 5, only mean values for R, averaged over foil thickness at each projectile energy are given in Fig. 6. We notice that generally $R_b < R_f < 1$ at the projectile energies used here.

In the following, the results will be compared to electronic stopping powers for molecules. First, data for the foil entrance (where the projectiles clearly are not oriented) will be discussed, and next, foil-exit data (where the projectiles may be partly aligned) are discussed.

The electronic stopping powers for nonoriented molecular projectiles seem to show some molecular enhancement in the projectile velocity region of interest here. This has been observed experimentally (Ref. 32), and a theoretical work based on Monte Carlo calculations (Ref. 33) indicate that for initially randomly oriented molecular projectiles, only enhanced molecular electronic stopping powers can be expected.

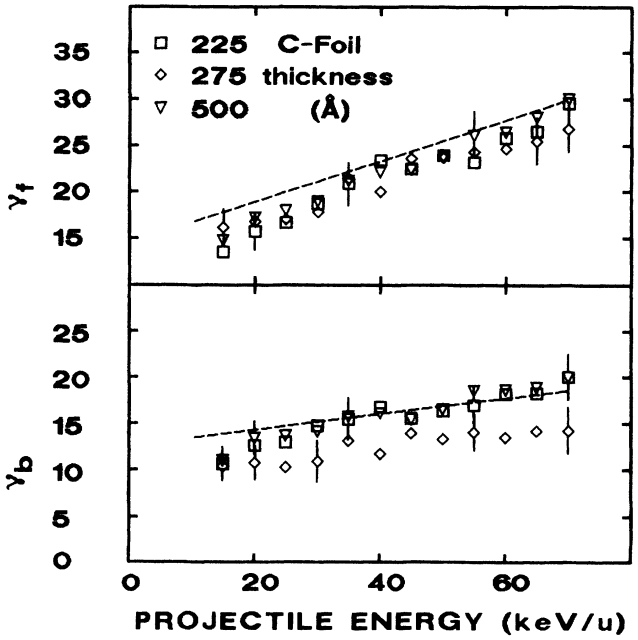

FIG. 4. The upper part of the figure shows γ_f vs projectile energy per nucleon for CO^+ on carbon foils of various thicknesses. For comparison the sum of γ_f produced by C^+ and O^+ (dashed line) is also shown. The lower part of the figure shows corresponding data for γ_b. Typical error bars are drawn.

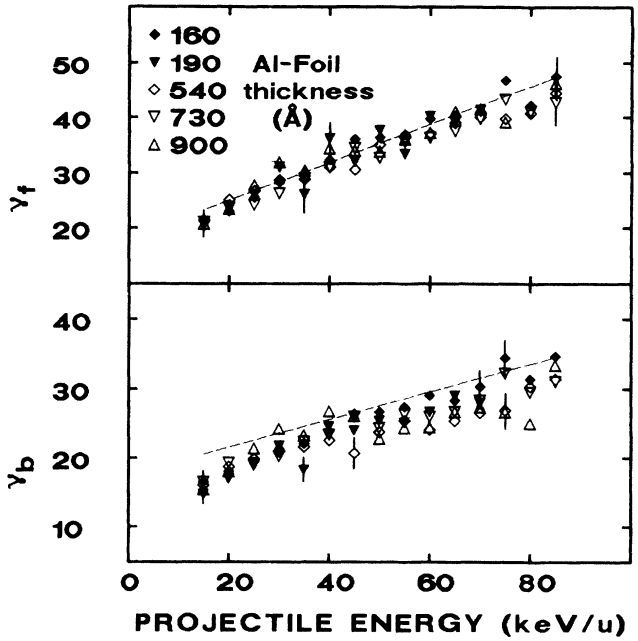

FIG. 5. The upper part of the figure shows γ_f vs projectile energy per nucleon for CO^+ on aluminum foils of various thicknesses. For comparison the sum of γ_f produced by C^+ and O^+ (dashed line) is also shown. The lower part of the figure shows corresponding data for γ_b. Some typical error bars are drawn.

In our measurements, the projectiles were initially not oriented, so that at the entrance of the foil an enhancement of the electronic stopping power would be expected. Despite this, the data for R_b show molecular reductions, see Fig. 6. The Monte Carlo calculations give $R > 1$, but they do not take into account the screening of the projectile charge by the binding electrons, which are assumed to be lost at the very entrance of the foil. So, they might not be very accurate, in particular, for the low velocities used in our experiment. Furthermore, energy-loss measurements always give an integral measure over the whole target thickness, whereas γ_b is a probe for what happens in the first few Å of the foil, depending on the escape depth λ_e of the SE. Within this thickness, the binding electrons have the chance to survive, screening the projectile charge and possibly leading to a smaller energy loss and SE yield before they are stripped off. As soon as they are lost, the cluster particles will suffer energy loss with their full charge, which then can lead to an enhanced stopping power, as discussed above. Additionally, in recent works, where monoatomic heavy ions were used in the same energy region as here, it was found that the proportionality between γ and dE/dx seems not to be strictly fulfilled for heavy projectiles at velocities near the Bohr velocity (Refs. 11 and 12).

During the passage through the foil, a fraction of the

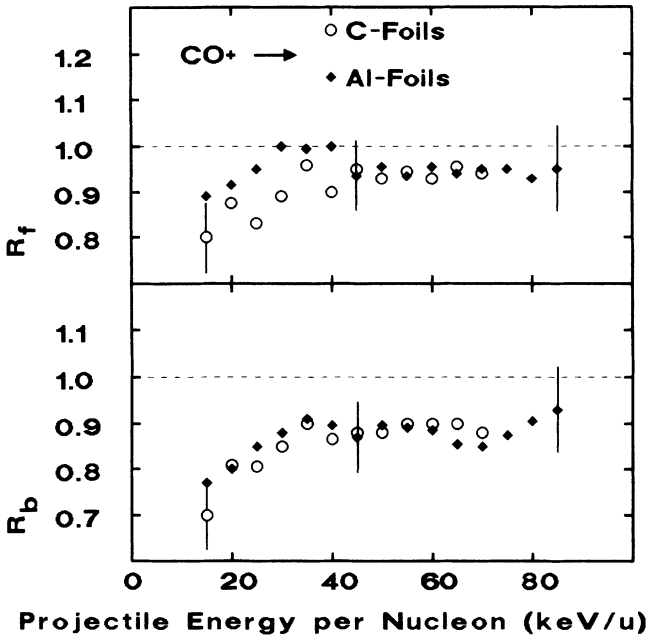

FIG. 6. The upper part of the figure shows R_f for CO^+ on carbon foils and aluminum foils vs the projectile energy per nucleon. For each projectile energy, only values averaged over the different foil thicknesses (cf. Figs. 4 and 5) are shown. The lower part of the figure contains corresponding data for R_b. Typical error bars are drawn.

molecular ions may align their axis along the beam axis due to the wake effect.[16,47] Such projectiles suffer smaller energy loss (Ref. 31) and will stay together for rather long distances (some 10 nm), Ref. 30, in contrast to unaligned clusters. The presence of such aligned molecules may explain that we observe molecular reductions for R_f (Fig. 6). Yet, at the foil exit, a majority—if not all—of the projectiles will have undergone Coulomb explosion in the foil, so that their internuclear separations are larger than at the foil entrance. This will, of course, in any case further reduce the small molecular effect (whatever its nature may be) at the foil exit in comparison to the foil entrance, as we observe it. However, at present, no clear conclusion can be drawn concerning the molecular reduction of γ_f we observe, and further work with thinner targets is needed.

C. Possible explanations for the molecular effect

As mentioned in the introduction, in the kinetic SEE model, Ref. 1, the secondary electrons are produced from a combination of the following three steps.

(i) Transfer of kinetic energy from the projectile to some target electrons.

(ii) Transport of some electrons from the bulk towards the target surface.

(iii) Transmission of some of these electrons through the surface.

The presence of a molecular effect in our data indicates that a modification of at least one of the three steps (i)–(iii) takes place when two or more particles move through the solid as a cluster. The two latter processes (ii) and (iii) are given by target properties in the sense that if the initial kinetic-energy distributions resulting from step (i), even if caused by different projectiles, are the same, then the transport (ii) and the transmission (iii) will be the same. Consequently, the molecular effects we see seem to be related basically to step (i), i.e., the creation of internal SE.

Several possible processes can be discussed, which may give rise to this modification.

(i) The binding electrons are lost in the first layers of the solid and can then create additional SE or even be emitted themselves. This process may lead to an enhancement of γ_b if the binding electrons are lost within the escape depth of the SE (some 10 to 20 Å, see Refs. 21 and 44, and if they come into play in addition to the electrons carried by the monoatomic projectiles.[21,48]

(ii) As long as the binding electrons are not yet lost, they can additionally screen the projectile charge with regard to distant collisions or collective excitation of the electron plasma of the solid. This can lead to a decreased energy loss of the molecule in the first few Å of the solid and thus to a smaller γ_b. If some molecules survive over longer distances inside the solid, this may even lead to a decrease of γ_f.

(iii) When the binding electrons are lost, the effective charge of the cluster with regard to distant collisions will equal the sum of the effective charges of its monoatomic contituents, $q^2_{\text{eff, cl}} = (\sum q_{\text{eff, at}})^2$. Since, for the energy loss, the square of the effective charge is relevant, the energy loss which the cluster suffers in distant collisions will be larger than for the single, monoatomic projectiles.[27] This may increase the production of SE and lead to an increased SE yield in the backward direction, and as well in the forward direction of thin foils, where the cluster has not yet separated too much due to Coulomb explosion and multiple scattering (see Ref. 21). In contrast, with regard to close collisions, the atomic constituents of the cluster will act independently ($q^2_{\text{eff, cl}} = \sum q^2_{\text{eff, at}}$) and no molecular effect can be expected.[34]

(iv) If one of the cluster particles is caught in the wake potential of another, then it may suffer less energy loss than a free projectile. If such aligned clusters survive until the exit of the foil, which seems to be possible even for large distances,[31,33] this may lead to a decrease in γ_f.

The majority of these processes should be significant only at the entrance side of the foil and at the exit of rather thin foils (some 10 to 100 nm, depending on the projectile energy). The appearance of molecular effects for γ_f also for thick foils indicates that some not yet fully understood processes may play a role for SEE and more experimental data concerning SEE in connection with energy loss are needed to elucidate the problem.

The velocity dependence of our measured molecular to atomic SE yield ratios is similar to the cluster energy-loss ratio calculations by Brandt and Ritchie.[27,34] This qualitative agreement can be seen from Fig. 7, where the "molecular effect" parameter $R(\gamma_b)$ is plotted as a function of the projectile velocity v_p. The experimental results for CO^+ on C and Al from Fig. 6 (dotted lines) and for H_2^+ on various target materials from Fig. 3 (dashed

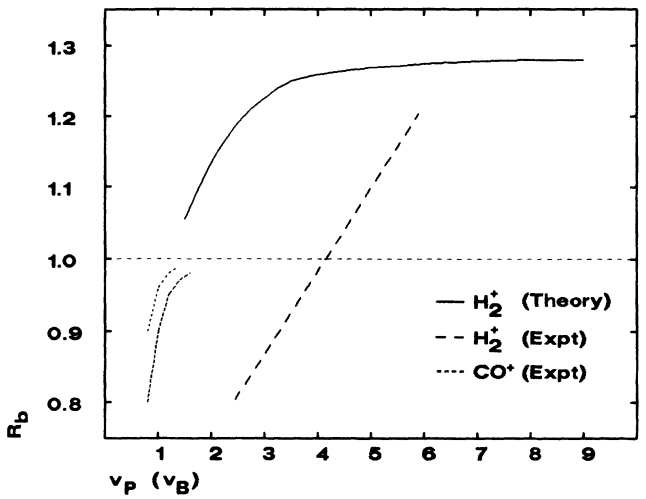

FIG. 7. Molecular effect parameter $R(\gamma_b)$ as a function of the projectile velocity v_p. The experimental results for CO^+ on C and Al targets from fig. 6 (upper and lower dotted lines, respectively) and H_2^+ on various target materials from Fig. 3 (dashed line) are compared to the theory of Brandt and Ritchie (Refs. 27 and 34) (solid line) for H_2^+ on C.

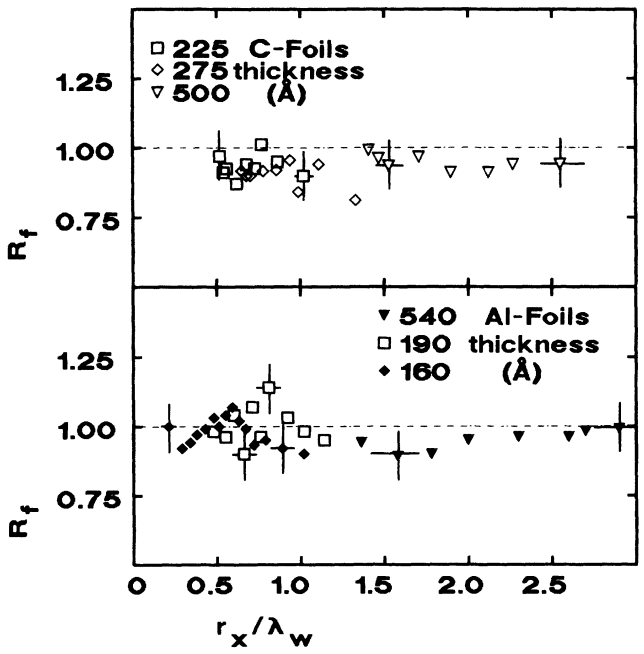

FIG. 8. The figure shows R_f for CO^+ on carbon (upper section) and aluminum (lower section) vs r_x/λ_w, see text. Typical error bars are drawn.

line) are compared to the cluster energy-loss theory of Brandt and Ritchie (Refs. 27 and 34) for H_2^+ on C. A slight increase of R with v_p is expected from the theory and is confirmed by the experimental results. However, at lower projectile velocities, we observed a yield reduction $R < 1$, and this is a new finding which is not included in present theories. The similar velocity dependence of the measured molecular-to-atomic SE-yield ratios and the energy-loss ratio calculations may indicate an approximate proportionality between γ and energy loss, also for molecular projectiles at velocities around and above the Bohr velocity.

However, simultaneous measurements of SE yields and the projectile energy loss are desirable, especially with molecular projectiles. Such experiments will help to clarify in which cases a proportionality between SE yields and energy loss (according to the Sternglass model[1]) exists.

In a previous experiment (Refs. 16 and 47), in which CO^+ projectiles and carbon foils were used and only the total SE yield γ_t was measured, an oscillatory structure was found for $R(\gamma_t)$ when plotted as a function of the ratio r_x/λ_w, where r_x is the internuclear distance and λ_w is the wake wavelength. The oscillations were explained as resulting from the superposition of the wake potentials of the two, Coulomb-exploding, molecular fragments when exiting the foil. The oscillations should therefore be more pronounced in our present measurements in which γ_f and γ_b have been recorded separately.

In Ref. 18, r_x was calculated regarding only the Coulomb explosion, and a target thickness dependent phase shift had to be introduced in order to fit a common oscillation for all data—a phase shift which accounted for the precise (Angstrøm-range) target thickness. We have calculated r_x with the Monte Carlo procedure described in Ref. 33, which includes Coulomb explosion, multiple scattering, and wake potential superposition. Figure 8 shows the results we obtained for R_f plotted versus r_x/λ_w. Within the uncertainty limits, there is no oscillatory behavior of R_f for the carbon foils.

Recently, it has been mentioned by Arista *et al.*[49] that the results of Refs. 16 and 47 can possibly be understood within cluster vincinage effects, as discussed above, and that it is not necessary to introduce Wake effects to understand these results. A closer inspection of our new aluminum data, however, indicates that an oscillation cannot be excluded for the thinnest targets. However, the amplitude of the oscillation is within the experimental uncertainty and is, therefore, not considered relevant. The reported oscillations in Refs. 16 and 47 may have likely been simulated by insufficient target thickness monitoring.

IV. CONCLUSION

We have measured the secondary electron yields in the forward (γ_f) and backward (γ_b) directions from thin C, Al, Ti, Ni, and Cu foils, induced by the molecular projectiles H_2^+, H_3^+, and CO^+ and their isotachic atomic constituents H^+, C^+, and O^+. At low projectile velocities ($v_p < 2v_B$), we observe a reduction, at higher velocities ($v_p > 4v_B$) an increase of the SE yields induced by the molecular projectiles compared to the sum of the yields induced by their isotachic atomic constituents.

We discuss these molecular effects in the frame of the Sternglass model[1] for kinetic emission of electrons, which divides the mechanism which leads to SEE into the three steps—production of internal SE, their transport to the surface, and finally their transmission. We conclude that the first step, the production, is the most sensitive one to

differences between molecular and atomic projectiles. It is influenced by the contribution of the binding electrons to the SE yield due to their additional production of SE as well as due to their screening of the projectile charge. The influence of the joint charges of the cluster particles on the energy loss of the cluster can furthermore affect the number and energy as well as spatial distribution of the internally produced SE.

However, the interplay of these different processes makes it difficult to determine how they act individually or whether yet other processes are involved. Further experiments with thinner targets, especially with simultaneous SE-yield and energy-loss measurements, are clearly needed to elucidate these problems. The similar velocity dependence of our measured molecular-to-atomic SE-yield ratios and Brandt's energy-loss-ratio calculations seem to indicate an approximate proportionality between γ and energy loss, also for molecular projectiles at velocities around and above the Bohr velocity. If this can be confirmed, SE-yield measurements may become a useful tool for the determination of energy loss in cases where energy-loss measurements are not easily applicable.

ACKNOWLEDGMENTS

One of us (E.V.) is grateful to the Institut für Kernphysik in Frankfurt am Main for the great hospitality he enjoyed during his stay as well as for financial support from the Julie Damms Foundation. This work has been supported by the German Bundesminister für Forschung und Technologie under Contract No. 060F173 /2 Ti476.

*Permanent address: Physics Laboratory, University of Copenhagen, Universitetsparken 5, DK-2100 Copenhagen, Denmark.

†Permanent address: Department of Electrical Engineering, Aristotelian University of Thessaloniki, GR-54006 Thessaloniki, Greece.

[1]E. J. Sternglass, Phys. Rev. **108**, 1 (1957).

[2]G. Holst and E. Oosterhuis, Physica (Utrecht) **1**, 82 (1921); H. D. Hagstrum, Phys. Rev. **97**, 325 (1954); in *Electron and Ion Spectroscopy of Solids,* edited by L. Fiermans, J. Vennik, and W. Dekeyser (Plenum, New York, 1978), p. 273.

[3]G. Holmén, B. Svensson, J. Schou, and P. Sigmund, Phys. Rev. B **20**, 2247 (1979).

[4]R. A. Baragiola, E. V. Alonso, and A. Oliva-Florio, Phys. Rev. B **19**, 121 (1979).

[5]E. V. Alonso, R. A. Baragiola, J. Ferrón, M. M. Jakas, and A. Oliva-Florio, Phys. Rev. B **22**, 80 (1980).

[6]A. Koyama, T. Shikata, and H. Sakairi, Jpn. J. Appl. Phys. **20**, 65 (1981).

[7]A. Koyama, T. Shikata, H. Sakairi, and E. Yagi, Jpn. J. Appl. Phys. **21**, 586 (1982).

[8]H. J. Frischkorn, K. O. Groeneveld, D. Hofmann, P. Koschar, R. Latz, and J. Schader, Nucl. Instrum. Methods **214**, 123 (1983).

[9]C. R. Shi, H. S. Toh, D. Lo, R. P. Livi, M. H. Mendenhall, D. Z. Zhang, and T. A. Tombrello, Nucl. Instrum. Methods **B9**, 263 (1985).

[10]C. C. Dednam, S. Froeneman, D. W. Mingay, and J. van Waart, Nucl. Instrum. methods **B24**, 366 (1987).

[11]H. Rothard, K. Kroneberger, M. Burkhard, J. Kemmler, P. Koschar, O. Heil, C. Biedermann, S. Lencinas, N. Keller, P. Lorenzen, D. Hofmann, A. Clouvas, K. O. Groeneveld, and E. Veje, Radiat. Eff. Def. Solids **109**, 281 (1989).

[12]H. Rothard, K. Kroneberger, P. Lorenzen, A. Clouvas, E. Veje, N. Keller, J. Kemmler, and K. O. Groeneveld, Phys. Rev. A (to be published).

[13]A. Clouvas, H. Rothard, M. Burkhard, K. Kroneberger, R. Kirsch, P. Misaelides, A. Katsanos, C. Biedermann, J. Kemmler, and K. O. Groeneveld, Phys. Rev. B **39**, 6316 (1989).

[14]D. Hasselkamp, Comments At. Mol. Phys. **21**, 24 111 (1988).

[15]J. E. Borovsky, D. J. McComas, and B. L. Barraclough, Nucl. Instrum. Methods **B30**, 191 (1988).

[16]H. J. Frischkorn and K. O. Groeneveld, Phys. Scr. **T6**, 89 (1983).

[17]D. Hasselkamp, K. G. Lang, A. Scharmann, and N. Stiller, Nucl. Instrum. Methods **180**, 349 (1981).

[18]B. Svensson and G. Holmén, Phys. Rev. B **25**, 3056 (1982).

[19]E. Veje, Nucl. Instrum. Methods **194**, 433 (1982).

[20]D. Hasselkamp and A. Scharmann, Phys. Lett. **96A**, 259 (1983).

[21]K. Kroneberger, A. Clouvas, G. Schlüssler, P. Koschar, J. Kemmler, H. Rothard, C. Biedermann, O. Heil, M. Burkhard, and K. O. Groeneveld, Nucl. Instrum. Methods **B29**, 621 (1988).

[22]D. Maor, P. J. Cooney, A. Faibas, E. P. Kanter, W. Koenig, and B. J. Zabranski, Phys. Rev. A **32**, 105 (1985).

[23]M. J. Gaillard, J. C. Poizat, A. Ratkowski, J. Remillieux, and M. Auzas, Phys. Rev. A **16**, 2323 (1977).

[24]R. Schramm, D. Hofmann, P. Koschar, H. J. Frischkorn, J. Kemmler, E. Rohrbach, and K. O. Groeneveld, Il Nuovo Cimento **7D**, 203 (1986).

[25]Y. Baudinet-Robinet, P.-D. Dumont, H. P. Garnir, and E. Veje, Nucl. Instrum. Methods **B13**, 175 (1986); E. Veje, J. Phys. B **21**, L255 (1988).

[26]K. O. Groeneveld, G. Astner, S. Hultberg, S. Mannervik, and P. S. Ramanujam, J. Phys. B **13**, L205 (1980).

[27]W. Brandt, A. Ratkowski, and R. H. Ritchie, Phys. Rev. Lett. **33**, 1325 (1974).

[28]M. F. Steuer, D. S. Gemmell, E. P. Kanter, E. A. Johnson, and B. J. Zabransky, Nucl. Instrum. Methods **194**, 277 (1982).

[29]J. C. Eckhardt, G. Lantschner, N. R. Arista, and R. A. Baragiola, J. Phys. C **11**, L851 (1978).

[30]N. R. Arista, Phys. Rev. B **18**, 1 (1978).

[31]M. F. Steuer, D. S. Gemmel, E. P. Kanter, E. A. Johnson, and B. J. Zabransky, IEEE Trans. Nucl. Sci. **NS30**, 1069 (1983).

[32]J. W. Tape, W. M. Gibson, J. Remillieux, R. Lauberti, and H. F. Wegner, Nucl. Instrum. Methods **132**, 75 (1976).

[33]J. Kemmler, P. Koschar, M. Burkhard, and K. O. Groeneveld, Nucl. Instrum. Methods **B12**, 62 (1985).

[34]W. Brandt and R. H. Ritchie, Nucl. Instrum. Methods **132**, 43 (1976).

[35]D. Hasselkamp. S. Hippler, A. Scharmann, and K.-H. Schartner, Z. Phys. D **6**, 269 (1987).

[36]J. Schou, Scanning Micros. **2**, 607 (1988).

[37]J. Hölzl and K. Jacobi, Sur. Sci. **14**, 351 (1969).

[38]M. Burkhard, W. Lotz, and K. O. Groeneveld, J. Phys. E **21**,

759 (1988).

[39]*Atomic and Molecular Collision Cross Sections of Interest in Controlled Thermonuclear Research,* edited by C. G. Barnett, J. A. Ray, and J. C. Thompson (Oak Ridge National Laboratory, Tenessee, 1964).

[40]M. Burkhard, H. Rothard, J. Kemmler, K. Kroneberger, and K. O. Groeneveld, J. Phys. D **21**, 472 (1988).

[41]H. Rothard, M. Burkhard, C. Biedermann, J. Kemmler, P. Koschar, K. Kroneberger, O. Heil, D. Hofmann, and K. O. Groeneveld, J. Phys. C **21**, 5033 (1988).

[42]P. Lorenzen, H. Rothard, K. Kroneberger, J. Kemmler, M. Burkhard, and K. O. Groeneveld, Nucl. Instrum. Methods **A282**, 213 (1989).

[43]W. Meckbach, G. Braunstein, and N. Arista, J. Phys. B **8**, L344 (1975).

[44]P. Koschar, K. Kroneberger, A. Clouvas, R. Schramm, M. Burkhard, O. Heil, J. Kemmler, H. Rothard, H.-D. Betz, and K. O. Groeneveld, Phys. Rev. A **40**, 3632 (1989).

[45]A. Clouvas, M. J. Gaillard, A. G. de Pinho, J. C. Poizat, J. Remillieux, and J. Desesquelles, Nucl. Instrum. Methods **B2**, 273 (1984).

[46]R. Levi-Setti, K. Lam, and T. R. Fox, Nucl. Instrum. Methods **194**, 281 (1982).

[47]H. J. Frischkorn, K. O. Groeneveld, P. Koschar, R. Latz, and J. Schader, Phys. Rev. Lett. **49**, 1671 (1982).

[48]D. Hasselkamp, S. Hippler, and A. Scharmann, Nucl. Instrum. Methods **B2**, 475 (1984).

[49]N. R. Arista, M. M. Jakas, G. H. Lantschner, and J. C. Eckardt, Phys. Rev. A **34**, 5112 (1986).